Available online at www.sciencedirect.com

ScienceDirect

Ceramics International 40 (2014) 12171–12177

CERAMICS INTERNATIONAL

www.elsevier.com/locate/ceramint

Synthesis and optical characterization of aluminum doped ZnO nanoparticles

A.N. Mallika*, A. RamachandraReddy, K. SowriBabu, K. Venugopal Reddy

Department of Physics, Materials Science Laboratory, National Institute of Technology, Warangal 506004, Andhra Pradesh, India

Received 15 February 2014; received in revised form 10 April 2014; accepted 10 April 2014
Available online 18 April 2014

Abstract

This paper reports on the structural and optical properties of Al doped ZnO nanoparticles prepared through a sol–gel method. Different atomic ratio's of Al were doped into ZnO ranging from 1 at% to 6 at%. X-ray diffraction (XRD) and FE-SEM results showed that the average crystallite size of ZnO nanoparticles decreased with increasing Al concentration. A compressive strain induced in ZnO with Al doping was calculated using *W–H* plot analysis. The band gap increased monotonously as Al concentration was increased from 1 at% to 6 at%. ZnO nanocrystals showed an emission peak positioned at 396 nm. The intensity of this peak decreases with Al doping for all concentrations. The decrease of the intensity of 396 nm emission peak is due to the worsening of the crystal quality due to Al doping. In addition to this, another peak at 437 nm is developed with Al doping and it is speculated to be due to the zinc interstitial defects.

Keywords: C. Optical properties; Al doped ZnO nanoparticles; Sol–gel method; X-ray diffraction

1. Introduction

Zinc oxide (ZnO) is one of the II–VI group compound semiconductors which crystallize in wurtzite structure belonging to the space group $P6_3mc$. It has characteristics of high transparency in visible range, good light trapping, low resistivity, non-toxicity, natural abundance, etc. which are important properties of optoelectronic and piezoelectric materials [1,2]. It has a direct band gap of 3.37 eV with a large exciton binding energy of 60 meV which ensures stable exciton emission even at room temperature. These unique properties make ZnO an important optoelectronic material due to its strong quantum confinement effects in experimentally suitable conditions. Iskandar [3] reported that, some nanoparticles (NPs) exhibited unique optical properties with a range of refractive indeces, high transparency, novel photoluminescence and plasmon resonance, etc. These can find potential applications such as catalysts, drug carriers, sensors, pigments, magnetic and optical materials and also in bio imaging, etc. [3]. For obtaining desired optical properties, preparation of ZnO nanoparticles (NPs) of different nanostructures such as 1D (Wires, fibers and rods), 2D (monolayer particle film), and 3D (ordered porous films) have become the intensive focus of research. ZnO NPs with controlled size and structure have size dependent properties in diverse areas of nanotechnology. It was reported recently that, powders, films, and ceramics of ZnO have been finding use in a scintillation technique [4]. Owing to these properties, it is considered as one of the most promising semiconductor for electronic, photonic, optical and biological applications [5]. The only disadvantage of ZnO is that it has high electrical resistivity which can be reduced by doping with III group elements [6]. Doping of ZnO by replacing Zn^{2+} with high valence atoms such as Ga, Al and also In, can in general induce dramatic changes in its electric as well as optical properties [7]. Among these metals, Al doped in ZnO (AZO)was considered as a promising candidate for improving its opto-electronic properties. Undoped ZnO usually contains various defects such as oxygen vacancies, zinc interstitials and also antisites 'O' (O_{zn}), etc. which would greatly affect the properties of ZnO. Hence by introducing Al as dopant, the defects environment is changed by means of substituting some Zn sites or occupying the interstitial sites by atoms of Al which in turn results in tunable band gap [1–8]. Zhou et al. [9] reported that Al doped zinc oxide coating exhibited high transparency and low resistivity which was suitable for fabrication

*Corresponding author. Tel.: +91 870 2462593; fax: +91 870 2459547.
E-mail address: mallika.nitw@gmail.com (A.N. Mallika).

http://dx.doi.org/10.1016/j.ceramint.2014.04.057
0272-8842/

of transparent electrodes in solar cells, gas sensors and also for ultrasonic oscillators [9]. The AZO is one of the best alternative materials to tin oxide and indium tin oxide not only in terms of cost but also in terms of non-toxicity, and posses comparable electrical and optical properties [9]. Therefore, it is felt better to investigate systematically the doping effect of Al on ZnO NPs. The effect of the dopant concentrations on the properties of semiconducting nanoparticles is very important from the point of view of basic physics as well as their potential applications. In general, NPs after preparation tend to agglomerate, as a result of it, the surface to volume ratio decreases and hence there is a decrease in ZnO sensitivity. The problem of agglomeration can be minimized by employing capping agent or surfactants like diethanolamine (DEA), polyvinyl alcohol (PVA), and ethylene glycol (EG) in the process of reactions; albeit their rate of reactions are to be lowered for well controlled and decreased nucleation process. As network template, PVA can control ZnO nucleation and crystal growth. For this purpose, PVA as surfactant was used. Recently, it was reported that ZnO prepared using polyvinyl alcohol showed very interesting PL property which changes with excitation wavelength [10].

The aim of the present work is to evaluate, the effect of Al doping in ZnO, in particular, on structural and optical properties of ZnO nanoparticles. Generally, in literature reports, it is stated that with Al doping of ZnO, it exhibited a red shift in the absorption peaks or decrease in the band gap which is not observed in the present study, may be because of the method of synthesis or due to the change of proper chelating agent etc.

2. Experimental procedure

Zinc nitrate hexahydrate (Zn $(NO_3)_2$ $6H_2O$), aluminum nitrate hexahydrate (Al $(NO_3)_2$ $6H_2O$) and PVA were used as starting chemicals for synthesis of $Al_xZn_{1-x}O$. All the chemical ingredients are AR grade of HI-Media and were weighed in stoichiometric proportions for getting 5 g of final product and were prepared as described elsewhere [11]. One of these samples was left undoped, whereas in the remaining samples, aluminum concentrations were varied with $x=1$ at%, 2 at%, 3 at%, 4 at%, and 6 at% of Al in $Al_xZn_{1-x}O$, and were named as Undoped, AZO1, AZO2, AZO3, AZO4, and AZO6, respectively.

The structural analysis of samples was carried out by using X-ray diffraction (XRD) recorded on a INEL XRG 3000 powder diffractometer equipped with CoKα radiation ($\lambda=1.7889$ Å) in terms of 2θ ranging from 20° to 120°. The morphology and grain size distribution of Al doped ZnO were investigated using a FE-SEM (Model: FESEM-SIRION). Sample contact to the electrodes was made by sputtering the sample with gold nanoparticles for 1 min using a sputtering instrument (Model: JEOLl JFC 1100E). From the FTIR (Model: PerkinElmer Spectrum-100) spectrum, recorded in the wave number range of 4000–400 cm^{-1}, the formation of ZnO was confirmed. Absorption spectra of samples were acquired using UV–visible spectrophotometer (Model: Thermo Scientific, evolution 600UV–vis) in the wavelength region of 250–450 nm. Finally, PL measurements were performed on a Jobin yuon spectrofluorometer (Model: Fluorolog-Fl3-11) with wavelength resolution of 0.2 nm at room temperature. A Xenon arc lamp of 450 W was used as the excitation light source to record the emission spectra of samples.

3. Results and discussion

3.1. XRD analysis

The XRD patterns of ZnO nanoparticles doped with different Al concentrations are shown in Fig. 1. The diffraction peaks corresponding to planes (100), (002), (101), (102), (110), (103), (112), and (201) confirmed the hexagonal wurtzite structure of ZnO nanoparticles [12]. No other secondary phase of oxides of Al or metallic Al was observed, indicating that Al is present in X-ray in an amorphous state [13]. The continuous increase in broadening of the XRD signals with increasing concentrations of Al indicates that the crystallite size of nanoparticles decreases [14,1]. The average crystallite size (d_{avg}) of the prepared samples was estimated from the width of diffraction peaks in the XRD spectrum using the Scherrer's equation [15].

$$d_{xrd} = \frac{0.9\lambda}{\beta \cos \theta} \quad (1)$$

where $\beta = \sqrt{\beta^2_{FWHM} - \beta^2_0}$ is the peak broadening after removing the instrumental broadening, $\beta_{(FWHM)}$ is the full width at half maximum and β_0 is the correction factor (0.007 rad). The average crystallite size calculated using Debye Scherrer's formula, in case of undoped sample is 32 nm, whereas for Al doped samples of AZO1, AZO2, AZO3, AZO4 and AZO6, they were 23 nm, 16 nm, 13 nm, 12 nm and 8 nm, respectively. By increasing doping concentrations, the intensity of peaks monotonously decreased with simultaneous increase in the FWHM. This indicates that the crystallinity deteriorated with increasing doping concentrations. With reference to the pristine ZnO peak, there is a slight shift observed in Al doped ZnO peak positions to higher angles may be because of incorporation of Al induced shift in the diffraction peak position to higher angles due to smaller atomic radii of Al. Since there is a difference in the ionic radii of the Zn^{2+} (0.60 Å) and Al^{3+} (0.39 Å), incorporation of Al ions in ZnO lattice probably

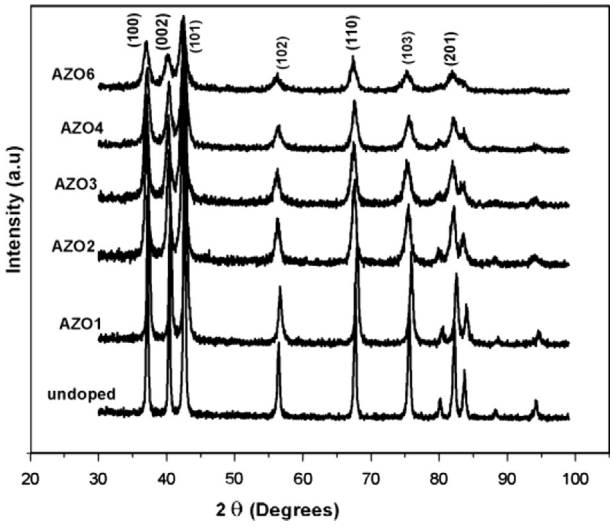

Fig. 1. XRD patterns of undoped and Al doped ZnO NP'S.

substituting Zn ion sites might have produced a compressive strain in the lattice [1]. *W–H* analysis is made to evaluate the strain induced broadening of peaks. The average crystallite size and strain in nanoparticles were calculated from the spectral line shape using Williamson–Hall (*W–H*) plot based on the following equation [16].

$$\frac{\beta \cos \theta}{\lambda} = \frac{0.9}{d} + \frac{4\varepsilon \sin \theta}{\lambda} \quad (2)$$

where β is the full width at half maximum, ε is the lattice strain, θ is the Bragg angle, d is the average crystallite size and λ is the wavelength of X-rays. The plot drawn between $(\beta \cos\theta)/\lambda$ and $(4\sin\theta)/\lambda$ gave rise to a straight line graph with a positive intercept as shown in Fig. 2(a). The strain is calculated from the slope of the linear fit and the y-intercept gives the inverse crystallite size. The crystallite sizes estimated from *W–H* plots followed the same trend as in the case of crystallite sizes based on Scherrer's formula. It is observed from the *W–H* analysis that, the induced strain increased for increasing concentrations of Al ranging from 1 at % to 6 at% and is shown in Fig. 2 (b). This may be due to the lattice mismatch with increasing concentrations of Al in ZnO.

3.2. FE-SEM analysis

Fig. 3 shows the typical SEM micrographs of ZnO nanoparticles prepared with different nominal Al concentrations. The formation of the polyhedral morphology with uniform grains of all samples which are in the range of 100–500 nm size is clear from the micrographs. The average grain sizes of all samples were determined by counting sufficiently large number of grains for ensuring the accuracy. The average grain size of undoped and doped samples estimated is below 100 nm. The grain sizes of samples were reduced up to 2 at% of Al concentration and then grain sizes increased for the other concentrations. The decrease in the average grain size with Al doping can be attributed as the dopant element may act as a microstructural stabilizer for fine and uniform grains.

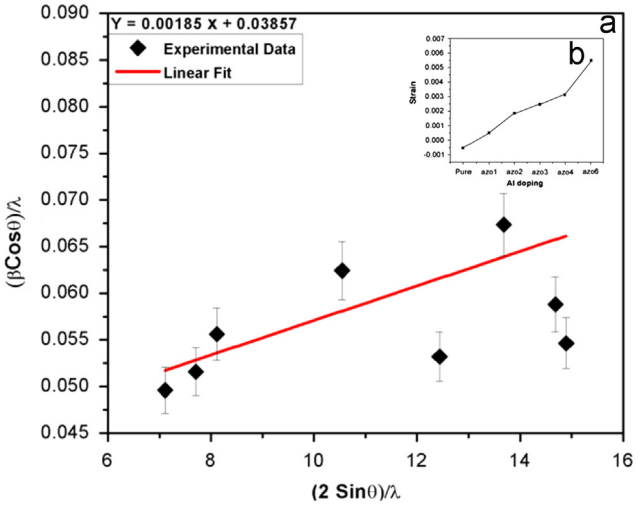

Fig. 2. (a). *W–H* Plot of AZO sample; Fig. 2(b) Strain versus Al concentration plot.

3.3. FTIR

FTIR is a technique used to obtain information about the chemical bonding and the elemental constituents of a material. The characteristic peaks exhibited by FTIR spectra of $Al_xZn_{1-x}O$ with $x=0$ at%, 1 at%, 2 at%, 3 at%, 4 at% and 6 at% are shown in Fig. 4. The broad absorption in the frequency band 3412 to 3456 cm^{-1} is assigned to O–H stretching vibration from H_2O in Zn–O lattice [17]. The peaks which are located at 2848 and 2933 cm^{-1} are due to symmetric and asymmetric C–H bonds, respectively [18]. An absorption band and a peak have been observed at about 2350 cm^{-1} and 1445 cm^{-1} respectively which arises from the absorption of atmospheric CO_2 on metal cations [19]. A sharp peak which appeared at about 683 cm^{-1} is a finger print of Al–O [17]. The peaks which appeared in the range of 550–437 cm^{-1} corresponds to the formation of Zn–O bond [20]. There is a shift observed in IR transmittance spectrum of Al doped ZnO, which may be ascribed to the crystal perturbation introduced by the dopant atoms into the lattice sites.

3.4. UV–vis analysis

The size of NP's plays an important role in changing entire properties of the nanomaterial. The UV–visible absorption spectroscopy is such a powerful technique to examine optical properties of semiconducting NP's [21]. In general, the UV absorption is related to the electronic transition from filled valence states to empty conduction states [22]. The absorption spectrum of AZO samples (Fig. 5(a)) exhibited a strong absorption peak in the vicinity of the absorption edge from 362 nm to 378 nm. Basically, this absorption can be attributed to the fundamental absorption of the exciton. It is seen from Fig. 5(b) that there is a blue shift in the peaks with simultaneous peak broadening with increasing Al doping concentration when compared to undoped ZnO which can be explained by the Moss–Burstein band filling effect. According to Moss–Burstein theory, the optical band gap of doped ZnO NPs is broader than undoped ZnO NP's [23]. Furthermore, it also explained that the lifting of the Fermi level into the conduction band of the degenerated semiconductor leads to the energy band broadening (blue shift) effect [24]. Thus, the low energy transitions are blocked with increase of Al concentrations, thereby filling the conduction band by electrons generally causing a blue shift in the band gap. The optical band gap of NP's was determined by using Tauc relationship [25] as given below:

$$\alpha h\upsilon = B(h\upsilon - E_g)^n \quad (3)$$

where α is the absorption coefficient, B is a constant, $h\upsilon$ is the energy of the incident photons, $n = 1/2$ for direct band gap semiconductors and E_g is the optical band gap. The band gap energy was calculated by extrapolation of the function $[F(\alpha h\upsilon)^2]$ versus $h\upsilon$ to zero as suggested by Weber [26] and as shown in Fig. 5(c). The optical band gaps of the undoped AZO1, AZO2, AZO3, AZO4, and AZO6 samples were estimated as 3.41 eV, 3.51 eV, 3.53 eV, 3.63 eV, 3.67 eV and 3.71 eV, respectively.

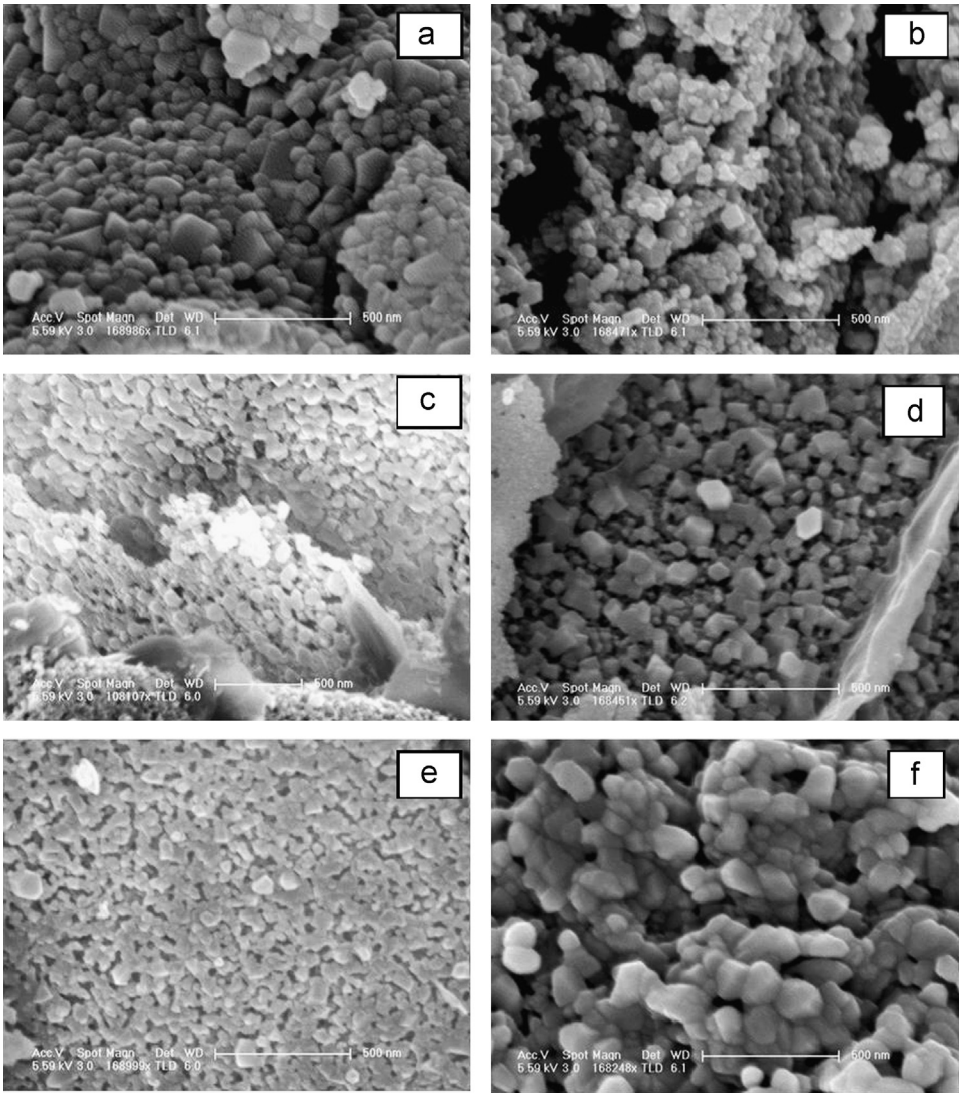

Fig. 3. Typical SEM micro graphs of (a) undoped (b) AZO1 (c) AZO2 (d) AZO3 (e) AZO4 and (f) AZO6 nano structures.

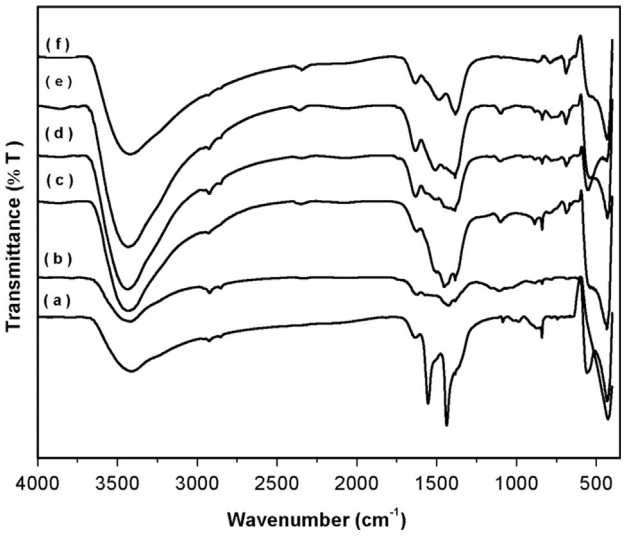

Fig. 4. FTIR spectrum of Al doped ZnO; (a) pristine ZnO sample, (b) AZO1, (c) AZO2, (d) AZO3 (e) AZO4, and (f) AZO6.

The band gap values increased with increasing concentrations of Al. This is in good agreement with the quantum confinement effects of nanoparticles [27]. According to quantum confinement theory, the energy band gap of a semiconductor depends on the crystallite size, i.e. its value will increase when there is a decrease in the crystallite size. Thus, the electronic structure of ZnO is significantly affected by Al incorporation.

3.5. Photoluminescence properties

Photoluminescence (PL) investigations are important to characterize a variety of material's parameters. The PL emission yields information on life time of excited states, identification of surface interface and impurity levels and intrinsic and extrinsic defects [28]. In PL spectra of ZnO, typically there are emission bands in the ultraviolet (UV) and visible (green, yellow, blue, and violet) regions. The ultraviolet emission is usually considered as the characteristic emission of ZnO, and is attributed to the band edge transition or the exciton recombination. For the green

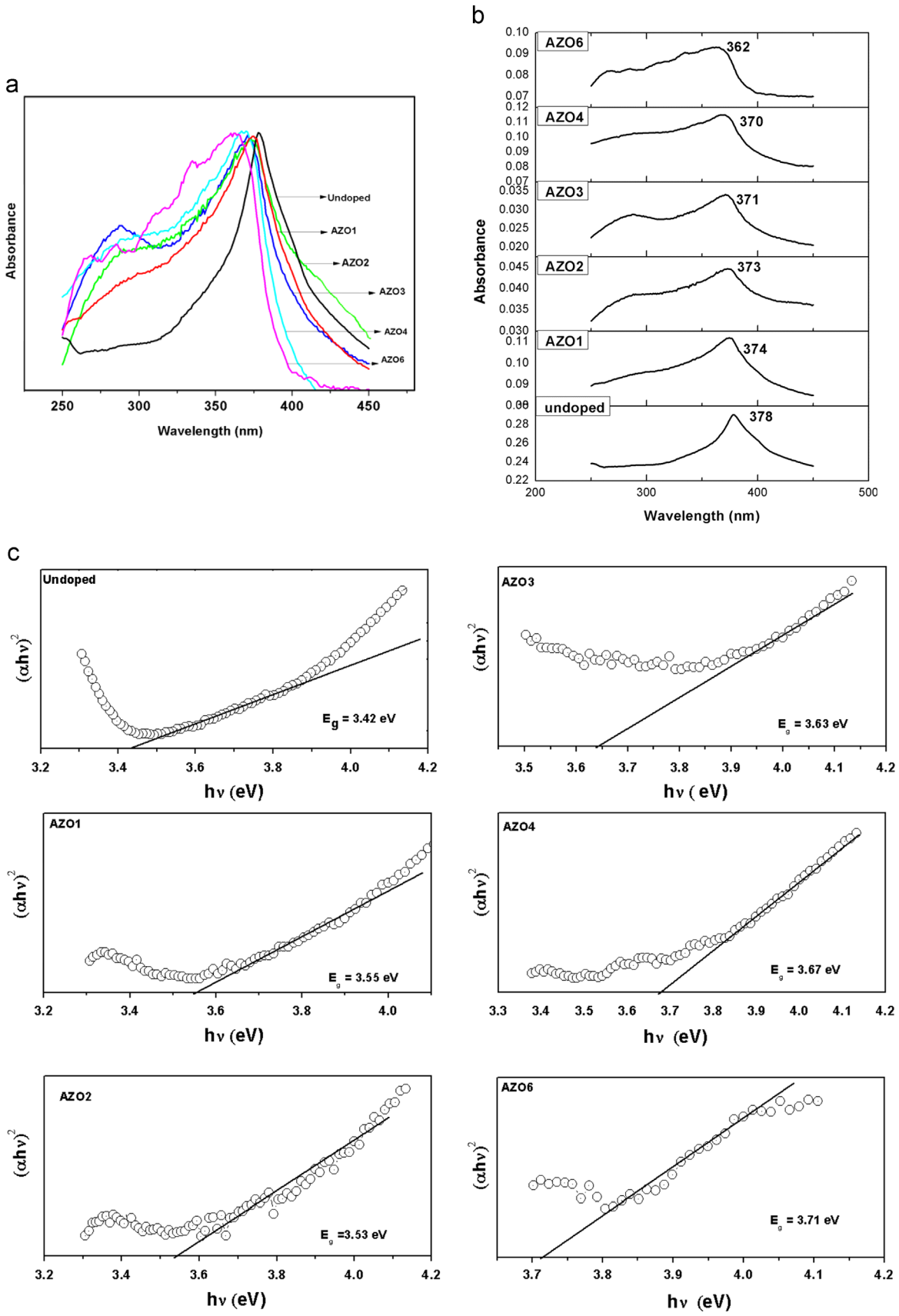

Fig. 5. (a). The UV–vis spectra of Undoped and Al doped ZnO samples. (b). The individual absorption peaks of all the samples. (c). The $(\alpha h\upsilon)^2$ vs $h\upsilon$ Tauc plots and the band gap energy estimation for undoped and Al doped ZnO nano particles.

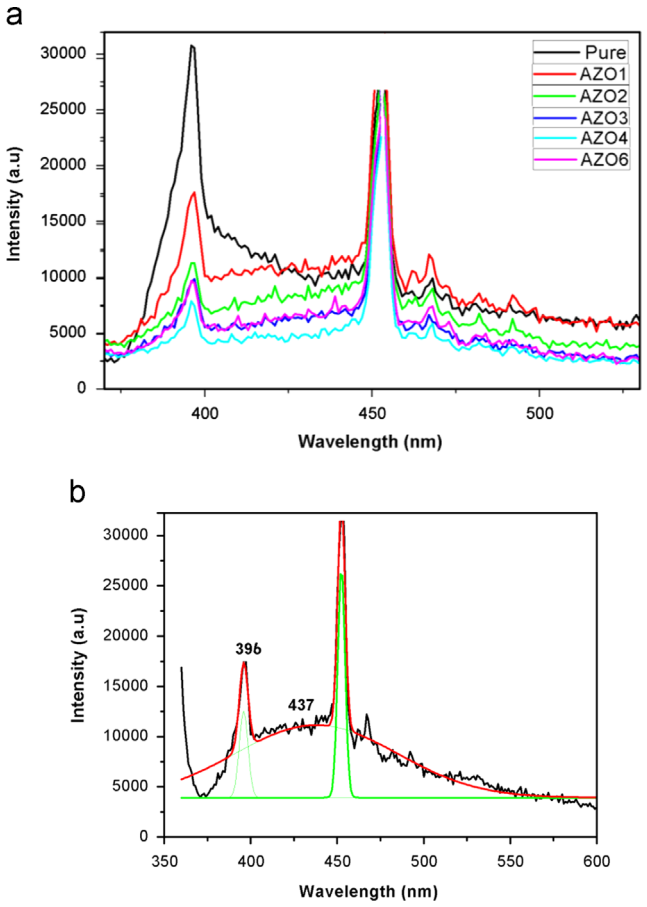

Fig. 6. (a). Room temperature PL spectrum of undoped and Al doped ZnO nanoparticles. (b). Gaussian deconvolution of the PL spectrum of ZnO nano particles containing 6 at. % of Al.

emissions, a number of different hypothesis have been proposed, such as transition between singly ionized oxygen vacancies and photoexcited holes, surface defects, oxygen interstitials, and zinc vacancies and extrinsic impurities, etc. which are considered as the origin [29–31]. In spite of extensive research on ZnO luminescence, the origin of green emission is still controversial. The PL spectra of Al doped ZnO samples recorded with an excitation wavelength at 353 nm are shown in Fig. 6(a). The pristine ZnO showed only UV emission peak positioned at 396 nm, whereas Al doped into ZnO, exhibited another peak at 437 nm in addition to 396 nm peak. The peak at 396 nm was attributed to the electron transition from the localized level slightly below the conduction band to the valence band [10]. The weakening of UV emission peak positioned at 396 nm may be attributed to the poor crystallinity upon increasing Al concentrations, as seen in the above XRD results. Further, a new peak positioned at 437 nm is developed with increasing Al concentration. Li and co-workers assigned the peak positioned at 437 nm to some defect states associated with Zn interstitials and oxygen vacancies [32]. Ngom et al. [33] and Chena et al. [34] assigned this blue emission peak to the electron transition from zinc interstitial level to the top of the valence band. In the present study, this 437 nm peak may be because of the strain induced defects with Al doping.

4. Conclusions

The AZO NPs were successfully synthesized by the sol–gel method with PVA as chelating agent. The effect of Al doping on the structural as well as optical properties were studied. The XRD patterns confirmed the formation of hexagonal wurtzite structure of ZnO. In addition, XRD results indicates that the crystallite size as well as the intensity of ZnO was influenced by Al doping. The average crystallite size of the samples decreased with increasing Al doping. The strain evaluated from *W–H* plot analysis exhibited an overall increase with Al doping concentration. This induced strain is reflected in the emission peaks also. The blue shift observed from UV–vis absorption spectrum with increase of Al doping, confirmed the quantum size confinement effects. It is also observed from the absorption peaks that peaks got broadened with increasing Al concentration. This can be explained as, the doping of Al induces defect levels with which, the transition from valence band to these defect levels broadened absorption peaks. There is an overall increase in the band gap of all the doped samples thereby exhibiting increased quantum size confinement effect with increase of Al doping. From the emission peaks, it became clear that, the intensity of the emission peaks monotonously decreased with Al doping, which was also observed in the XRD and absorption peaks. This can be attributed to defects which are generated with Al doping. Hence there is an extra emission peak generated at 437 nm with Al doping in emission peaks. Thus the feasibility of Al incorporation into ZnO implies the ability to control the crystallinity as well as tailoring of the band gap.

Acknowledgment

The authors are greatly thankful to MHRD, Govt. of India for the financial support through Institute fellowship for Ph.D. program. The authors wish to thank Mr. Rajasegaran E, Indian Institute of Sciences Bangalore (IISc) for helping in FE-SEM measurements and authors would also like to thank Mr. Y.B Ravishankar (University of Hyderabad) for his help in XRD measurements.

References

[1] R. SaravanaKumar, R. Sathyamoorthy, P. Sudhagar, P. Matheswaran, P. Hrudhya, Kang Yong Soo, Effect of aluminum doping on the structural and luminescent properties of ZnO nanoparticles synthesized by wet chemical method, Physica E 43 (2011) 1166–1170.
[2] Zhanchang Pan, X. Tian, Shoukun Wu, C. Xiao, Zhuliang Li, Jianfeng D, G. Hu, Z. Wei, Effects of Al and Sn dopants on the structural and optical properties of ZnO thin films, Superlattice Microstruct. 54 (2013) 107–117.
[3] Ferry Iskandar, Nanoparticle processing for optical applications : a review, Adv. Powder Technol. 20 (2009) 283–292.
[4] P.A. Rodnyi, I.V. Khodyuk, Optical and luminescence properties of zinc oxide, Opt. Spectrosc. 111, 776–785.
[5] Meghana Ramani, S. Ponnusamy, C. Muthamizhchelvan, Zinc oxide nanoparticles: a study of defect level blue–green emission, Opt. Mater. 34 (2012) 817–820.
[6] S.R. Aghdaee, V. Soleimanian, B. Tayebi, Effect of Al doping on the microstructural, optical and electrical properties of ZnO films, Superlattice Microstruct. 51 (2012) 149–162.

[7] C. Samanta, S. Albonett, L. Forni, F. Peri, Dario Lazzari, Solvothermal synthesis and properties control of doped ZnO nanoparticles, J. Colloid Interface Sci. 329 (2009) 73–80.
[8] Xu. Zi-qiang, Deng Hong, Li. Yan, Cheng Hang, Al-doping effects on structure, electrical and optical properties of c-axis-orientated ZnO: Al thin films, Mater. Sci. Semicond. Process. 9 (2006) 132–135.
[9] Hong-ming Zhou, Dan-qing Yi, Zhi-ming Yu, Lai-rong Xiao, Jian Li, Preparation of aluminum doped zinc oxide films and the study of their microstructure, electrical and optical properties, Thin Solid Films 515 (2007) 6909–6914.
[10] K. Sowri Babu, A.R.C. Reddy, Ch. Sujatha, K.V.G. Reddy, Optimization of UV emission intensity of ZnO nanoparticles by changing the excitation wavelength, Mater. Lett. 99 (2013) 97–100.
[11] A.N. Mallika, K. Sowri Babu, A. Ramachandra Reddy, Ch. Sujatha, K. Venugopal Reddy, Structural and photoluminescence properties of Mg substituted ZnO nanoparticles, Opt. Mater. 36 (2014) 879–884.
[12] Guang-hui Ning, Xiao-peng Zhao, Jia Li, Structure and optical properties of $Mg_xZn_{1-x}O$ nanoparticles prepared by sol–gel method, Opt. Mater. 27 (2004) 1–5.
[13] M. Behrens, G. Lolli, N. Muratova et al. The effect of Al-doping on ZnO nanoparticles applied as catalyst support, Phys. Chem. Chem. Phys. http://dx.doi.org/10.1039/c2cp41680h.
[14] H. Sonja, Moazzam Ali, S. Christof, M. Winterer, H. Wiggers, Electrical properties of aluminum-doped zinc oxide (AZO) nanoparticles synthesized by chemical vapor synthesis, Nanotechnology 20 (2009) 445701.
[15] B.D. Cullity, in: Elements of X-ray Diffractions, Addison-Wesley, 1978, p. 102.
[16] P.K. Giri, S. Bhattacharya, R. Kesavamoorthy, B.K. Panigrahi, K.G.M. Nair, Correlation between microstructure and optical properties of ZnO nanoparticles synthesized by ball milling, J. Appl. Phys. 102 (2007) 093515.
[17] N. Rajeshwari Y, A. Chandra Bose, Absorption-emission study of hydrothermally grown Al: ZnO nanostructures, J. Alloy Compd. 509 (2011) 8493–8500.
[18] M. Vafaee, M. Sasani Ghamsari, Preparation and characterization of ZnO nanoparticles by a novel sol–gel route, Mater. Lett. 61 (2007) 3265–3268.
[19] Imran Khan, Shakeel Kahn, Razia Nongjai, Hilal Ahmed, Wasi Khan, Structural and optical properties of gel-combustion synthesized Zr doped ZnO nanoparticles, Opt. Mater. 35 (2013) 1189–1193.
[20] S.S. Alias, A.B. Ismail, A.A. Mohamad, Effect of PH on ZnO nanoparticle properties synthesized by sol-gel centrifugation, J. Alloy Compd. 499 (2010) 231–237.
[21] T. Satyanarayana, K. SrinivasaRao, G. Nagarjuna, Synthesis, Characterization, and Spectroscopic Properties of ZnO Nanoparticles, ISRN Nanotechnol. (2012), http://dx.doi.org/10.5402/2012/372505.
[22] S. Suwanboon, P. Amornpitoksuk, A. Sukolrat, Dependence of optical properties on doping metal, crystallite size and defect concentration of M-doped ZnO nanopowders (M=Al, Mg, Ti), Ceram. Int. 37 (2011) 1359–1365.
[23] S. Suwanboon, P. Amornpitoksuk, A. Haidoux, J.C. Tedenac, Structural and optical properties of undoped and aluminum doped zinc oxide nanoparticles via precipitation method at low temperature, J. Alloy Compd. 462 (2008) 335–339.
[24] Z.Q. Xu, H. Deng, Y. Li, Q.H. Guo, Y.R. Li, Characteristics of Al-doped c-axis orientation ZnO thin films prepared by the sol–gel method, Mater. Res. Bull. 41 (2006) 354–358.
[25] S.A. Ansari, A. Nisar, B. Fatma, W. Khan, A.H. Naqvi, Investigation on structural, optical and dielectric properties of Co doped ZnO nanoparticles synthesized by gel-combustion route, Mater. Sci. Eng. B 177 (2012) 428–435.
[26] Robert S. Weber, Effect of local structure on the UV–visible absorption edges of molybdenum oxide clusters and supported molybdenum oxides, J. catal. 151 (1995) 470–474.
[27] Toshihide Takagahara, Kyozaburo Takeda, Theory of the quantum confinement effect on excitons in quantum dots of indirect-gap materials, Phys. Rev B 46 (1992) 15578.
[28] N. Jabena Begum, K. Ravichandran, Effect of source material on the transparent conducting properties of sprayed ZnO: Al thin films for solar cell applications, J. Phys. Chem. Solids 74 (2013) 841–848.
[29] Y.G. Wang, S.P. Lau, H.W. Lee, S.F. Yu, B.K. Tay, Photoluminescence study of ZnO films prepared by thermal oxidation of Zn metallic films in air, J. Appl. Phys. 94 (2003) 354.
[30] Haibo Zeng, Guotao Duan, Yue Li, Shikuan Yang, Xiaoxia Xu, Weiping Cai, Blue luminescence of ZnO nanoparticles based on non-equilibrium processes: defect origins and emission controls, Adv. Funct. Mater. 20 (2010) 561–572.
[31] U. Ozgur, Ya.I. Alivov, C. Liu, A. Teke, M.A. Reshchikov, S. Doan, V. Avrutin, S.-J. Cho, H. Morkoc, A comprehensive review of ZnO materials and devices, J. Appl. Phys. 98 (2005) 041301.
[32] L. Kumari, W.Z. Li, C.H. Vannoy, R.M. Leblanc, D.Z. Wang, Zinc oxide micro- and nanoparticles: synthesis, structure and optical properties, Mater. Res. Bull. 45 (2010) 190–196.
[33] B.D. Ngom, O. Sakho, N. Manyala, J.B. Kana, N. Mlungisi, L. Guerbous, A.Y. Fasasi, M. Maaza, A.C. Beye, Structural, morphological and photoluminescence properties of W-doped ZnO nanostructures, Appl. Surf. Sci. 255 (2009) 7314–7318.
[34] Haixia Chena, Jijun Ding, Wenge Guo, Effect of sputtering parameters on photoluminescence properties of Al doped ZnO films deposited on Si substrate, Ceram. Int. 40 (2014) 4847–4851.